J. Hydrol. Hydromech., 68, 2020, 2, 111–118
DOI: 10.2478/johh-2020-0007
ISSN 1338-4333

sciendo Journal of Hydrology and Hydromechanics

Simultaneous determination of wettability and shrinkage in an organic residue amended loamy topsoil

Steffen Beck-Broichsitter[1*], Saskia Ruth[2], Richard Schröder[2], Heiner Fleige[2], Horst H. Gerke[1], Rainer Horn[2]

[1] Research Area 1 "Landscape Functioning", Leibniz Centre for Agricultural Landscape Research (ZALF), Eberswalder Str. 84, 15374 Müncheberg, Germany.
[2] Institute of Plant Nutrition and Soil Science, Christian-Albrechts-University Kiel, Hermann-Rodewaldstr. 2, 24118 Kiel, Germany.
[*] Corresponding author. Tel.: +49 33432 82412. E-mail: steffen.beck-broichsitter@zalf.de

Abstract: In agricultural land use, organic residues such as compost, digestate, and sewage sludge are discussed as cost-effective soil conditioner that may improve the water holding capacity and crop available soil moisture. The objective of this study is to determine the effect of application of digestates with different compositions in maize, sugar beet and winter wheat, compost of shrub debris and sewage sludge on shrinkage behaviour and contact angle of till-derived loamy topsoil of a Haplic Luvisol under agricultural use. Novelty is the simultaneous determination of contact angle and shrinkage of soils amended with digestates composed of different composition in maize, sugar beet and winter wheat, compost of shrub debris and sewage sludge. The results suggest that the application of organic residues impacts the air capacity, while the contact angles remained in the subcritical range between > 0° and < 90°. The relationship between CA values and moisture ratios, ϑ, during proportional shrinkage was positive and linear (r^2 of 0.98) and negative during residual- and zero-shrinkage (r^2 of 0.93).

Keywords: Luvisol; Organic residues; Contact angle; Wettability; Shrinkage.

INTRODUCTION

Organic residues like aerobically composted or anaerobically digested organic materials and sewage sludge are used as organic fertilizers in agriculture (Risberg et al., 2017; Voelkner et al., 2015) and soil structure conditioner in post-mining landscapes (Beck-Broichsitter et al., 2018b).

Apart from the positive effects of the organic residues on soil properties and functions, the critical impact of organic residues, consisting of hydrophobic substances (humic fulvic or long-chained fatty acids) and hydrophobic functional groups (i.e., Ruggieri et al., 2008), on the soil wettability should also be considered. Interactions between organic matter-containing soil matrix and organic residues can modify soil wettability (i.e., Goebel et al., 2007), especially through volatile fatty acids containing anaerobically attended residues (Risberg et al., 2017) which cause hydrophobic soil conditions (Goebel et al., 2007). In particular, the adsorption of humic acids to mineral particles of sand-dominated soils with low specific surfaces results in higher contact angles and therefore an increase in hydrophobic behaviour (i.e., Wang et al., 2010).

Under dry conditions, the application of organic residues may decrease the wettability of topsoil surface due to an increased hydrophobicity of the soil organic matter (i.e., Vogelmann et al., 2013) that in combination with shrinkage-induced soil crack formation can enhance preferential flow (Gerke, 2006). When bypassing the lower permeable soil matrix through cracks (Bebej et al., 2017), the soil's filtering function is strongly reduced and preferentially transported organic residue solutes containing plant nutrients can negatively impact the ground water quality (Kodešová et al., 2012; Köhne et al., 2009), while at the same time the plant nutrient supply can be deficient.

The soil shrinkage curve is the relation between the void ratio, e, and the moisture ratio, ϑ, and can be divided into four characteristic stages: structural-, proportional-, residual-, and zero shrinkage (Braudeau, et al., 2004; Peng and Horn, 2005; Peng and Horn, 2013) and into a capillary-affected and an adsorption-affected region (i.e., Lu and Dong, 2016). The definition of residual- and zero-shrinkage is that the soil volume loss is negligibly smaller than the water volume loss (Beck-Broichsitter et al., 2018b; Braudeau et al., 2004). The residual- and zero-shrinkage phase in the range of low moisture ratios, ϑ, is of major interest for the contact angles, CA, and therefore the wettability of intact soil surfaces (Chen and Ning, 2018), because a reduced water adsorption capability of intact crack surfaces may intensify the preferential flow through shrinkage cracks (i.e., Kodešová et al., 2011; Leue et al., 2015).

The impact of organic residues and its organic matter composition on soil chemical properties has already been evaluated (i.e., Fér et al., 2016; Kodešová et al., 2011, 2012; Voelkner et al., 2015), and the application of for example compost can have a positive effect on air capacity and water holding capacity of soils (Beck-Broichsitter et al., 2018b), but a lack of information in case of the impact on physical properties and especially the shrinkage behaviour is still existing.

The objective of this study is to determine the effect of application of digestates with different compositions in maize, sugar beet and winter wheat, compost of shrub debris and sewage sludge on shrinkage behaviour and contact angle of till-derived loamy topsoil (Ap-horizon, 0–0.2 m depth) of a Haplic Luvisol under agricultural use.

The authors hypothesized that the application of organic residues on loamy topsoil can increase the air capacity and plant available water capacity, and can lower the shrinkage crack formation tendency and the contact angles especially in the low moisture ratio range.

MATERIALS AND METHODS

Sample preparation and laboratory analysis

Soil material was sampled from the topsoil (Ap-horizon, 0–0.2 m depth) of a Haplic Luvisol (Ap/E/Bt/Bw/C) (IUSS Working Group WRB, 2014), derived from glacial till, located at the research farm in Hohenschulen (54°31'28"N, 9°98'35"E), near Kiel (Schleswig Holstein) in Northern Germany. Organic residues in form of shrub-derived compost (C), sewage sludge (S), and three digestates consisting of (i) 80% maize and 20% sugar beet (80M20B), (ii) 20% maize and 80% sugar beet (20M80B), (iii) 20% winter wheat and 80% sugar beet (20W80B) were used for application to the till-derived loam (L).

At first, organic residues were air-dried, sieved (≤ 2 mm) and then mechanically mixed with the loam (θ of approx. 0.1 cm^3 cm^{-3}) to simulate the common annual application rates per hectare for fertilizer in 0.2 m topsoil with 30 Mg dry mass ha^{-1} for compost and 30 m^3 moist mass ha^{-1} for digestates and sewage sludge. After application of the organic residues, the organic carbon content, OC (g kg^{-1}), (by coulometric carbon dioxide measurement), soil texture (by combined sieve and pipette method), and soil pH values (in 0.01M $CaCl_2$ solution) were analysed for more details see Hartge and Horn (2016).

In a second step, the loam and loam-residue-mixtures were compacted to a dry bulk density, ρ_b, of 1.45 g cm^{-3} with a load frame (Instron 8871, Norwood, USA) with pressing force of 5 kN, resulting in 8–10 density-defined soil cores (diameter: 5.5 cm, height: 5 cm), each.

Contact angle measurements

The contact angle, CA, was determined by the sessile drop method through application of a water droplet on surfaces of soil cores with 8–10 repetitions for loam and loam-residue mixtures each for pressure heads, h, of –60 hPa, –300 hPa, –15000 hPa, and oven-dried at 105°C, respectively (Figure 1).

The CA was determined with CCD-equipped contact angle microscope (OCA 15, DataPhysics, Filderstadt, Germany) and the placement of 2 µg of water (5 repetitions on identic points per drying stage) was recorded by a highspeed camera allowing the evaluation of the CA (resolution: 0.1°) with SCA20 program (DataPhysics, Filderstadt, Germany). The contact angle, CA (°), was calculated following Bachmann et al. (2013) in the first five seconds after drop placement on the soil surface:

$$CA = \arccos\left(\frac{\sigma_S - \sigma_{SL}}{\sigma_L}\right) \quad (1)$$

where σ_S is the surface energy of the solid (J m^{-2}), σ_{SL} is the solid-liquid interfacial energy (J m^{-2}), and σ_L is the surface tension of the liquid (J m^{-2}). The CA can be classified as follows: CA = 0° indicates complete wettability of the surface, 0° > CA < 90° = subcritical, subhydrophilic material, CA > 90° = hydrophobic material and CA = 160° indicates super hydrophobic material (i.e., Lamparter et al., 2006).

Soil water retention and shrinkage measurements

The volumetric water content, θ, for the prepared soil cores with 8–10 repetitions for loam and loam-residue mixtures with ρ_b values of 1.45 g cm^{-3} each were determined by a combined pressure plate (saturated, –60, –300 hPa) and ceramic vacuum outflow method (–15000 hPa) as well as oven-dried for 24 hours at 105°C, respectively. Simultaneously, the soil volume change was determined with the 3D laser triangulation method (Beck-Broichsitter et al., 2018a, 2020; Seyfarth et al., 2012). In brief, the line laser CMS 106 with λ = 660 nm (Control Micro Systems, Orlando, FL, USA) illuminates a soil core along the cylindrical surface (rotation centre at the z-axis), depending on the scan area. During the rotation process, a CCD camera captures a predefined number of profiles, while the camera

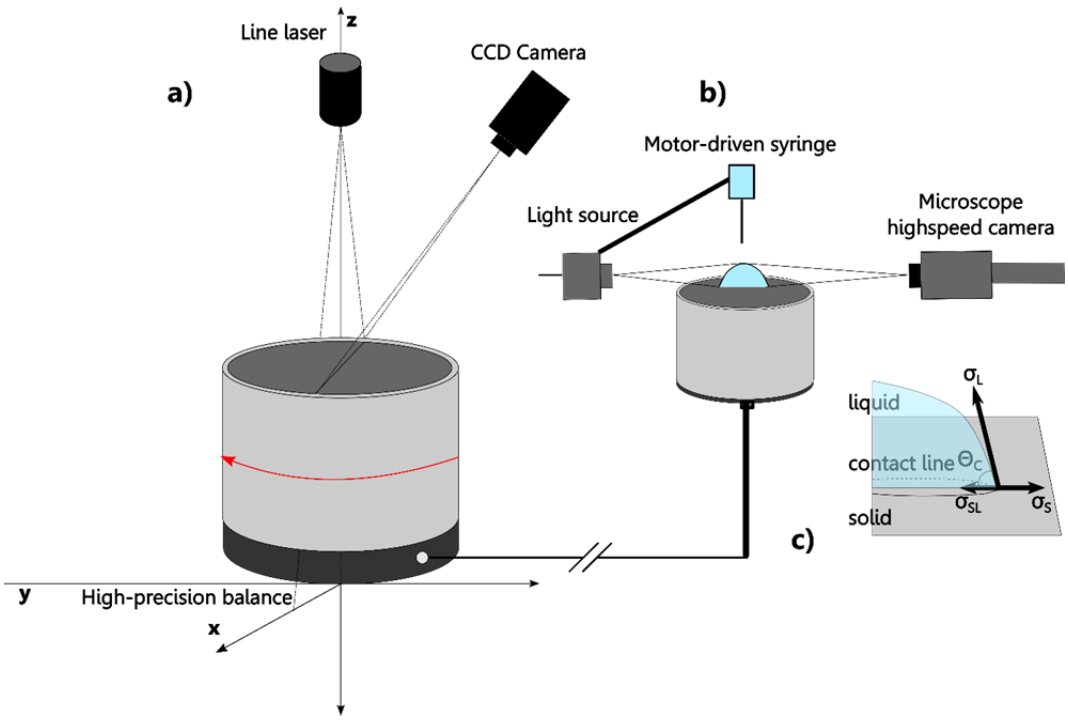

Fig. 1. Experimental setup for a) automatic determination of contact angle, CA, of intact soil surfaces through sessile liquid drop method, and b) concept of equlilibrium contact angle, Θ_C, and three-phase contact line between solid, liquid and gas phase.

is provided with a band-pass filter to segregate the laser signal (highlighted profile) in the captured image from the background (Figure 1).

The soil porosity, ε, was calculated as:

$$\varepsilon = 1 - \frac{\rho_b}{\rho_s} \quad (2)$$

where ρ_s is solid particle density and ρ_b the bulk density of the soil. For ρ_s, a value of 2.65 g cm^{-3} was assumed for the sand-dominated loamy soil. From the observed water retention data, the air capacity, AC (cm^3 cm^{-3}), and the plant available water capacity, AWC (cm^3 cm^{-3}), were calculated as follows:

$$AC = \varepsilon - \theta_{-60hPa} \quad (3)$$

$$AWC = \theta_{-60hPa} - \theta_{-15000hPa} \quad (4)$$

where $\theta_{-60\ hPa}$ and $\theta_{-15000\ hPa}$ correspond to the water content at pressure heads of –60 hPa and –15000 hPa.

The soil shrinkage curve is generally divided into four phases (Figure 2): structural-, proportional-, residual-, and zero shrinkage (i.e., Braudeau et al., 2004). The shrinkage limit points e_{ae} and ϑ_{ae} of Eq. (9) indicate the air entry point or rather the beginning of residual shrinkage. This means that the soil volume loss and decrease in void ratio, e, during dehydration is lower than the water volume loss and decrease in moisture ratio, ϑ, while zero-shrinkage describes a more or less remaining soil volume or void ratio in spite of decreasing moisture ratio (Peng and Horn, 2005, 2013).

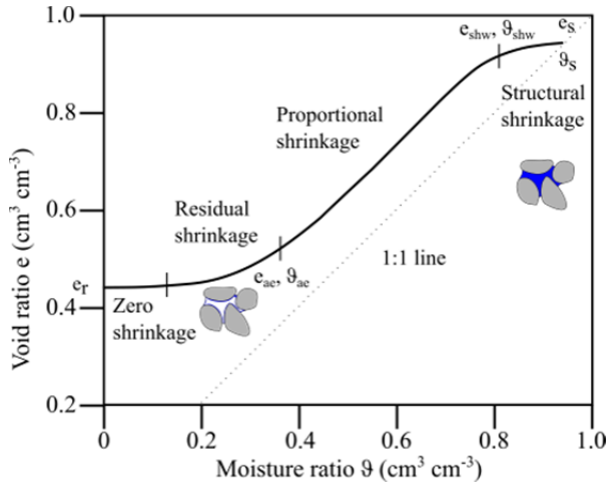

Fig. 2. Conceptual model of soil shrinkage curve with four characteristic shrinkage regions: structural-, proportional-, residual-, and zero shrinkage, while e_s and ϑ_s are the saturated void and moisture ratio, respectively, and e_r is the residual void ratio.

These soil shrinkage curves are defined by the relation between the void ratio, e (cm^3 cm^{-3}), and the moisture ratio, ϑ (cm^3 cm^{-3}), following Hartge and Horn (2016):

$$e = \frac{\rho_s}{\rho_b} - 1 \quad (7)$$

$$\vartheta = \rho_s \theta_m \quad (8)$$

where ρ_s, ρ_b, and θ_m are the particle and bulk density (g cm^{-3}), and gravimetric water content (g g^{-1}), respectively.

The model of Peng and Horn (2005) was selected in this study to describe the shrinkage curve as:

$$e(\vartheta) = \begin{cases} e_r & \vartheta = 0 \\ e_r + \dfrac{e_s - e_r}{\left[1 + (\chi\vartheta)^{-p}\right]^q} & 0 \le \vartheta \le \vartheta_s;\ n > 0 \\ e_s & \vartheta = \vartheta_s \end{cases} \quad (9)$$

where χ, p, and q are dimensionless fitting parameters, e_s and e_r are the saturated and residual void ratios, respectively, fulfilling the following boundary conditions:

$$\vartheta \to 0;\ \frac{\vartheta}{e_s - \theta} \to 0;\ e \to e_s \quad (10)$$

$$\vartheta \to \vartheta_s;\ \frac{\vartheta}{e_s - \vartheta} \to \infty;\ e \to e_s \quad (11)$$

The volume shrinkage index, ΔV, describes the shrinkage tendency of differently-textured soils as follows (Alaoui et al., 2011):

$$\Delta V = \frac{V_{0hPa}}{V_{105°C}} - 1 \quad (12)$$

where ΔV is the change in soil volume as relation between the quasi-saturated (0 hPa) and the dry stage (105°C), while ΔV < 5% corresponds to good, ΔV = 5–10% to medium, and ΔV > 10% to poor shrinkage tendency.

Statistical analysis

The statistical software R (R Development Core Team, 2014) was used to evaluate the data. The data were tested for normal distribution and heteroscedastic on the Shapiro-Wilk-Test and graphical residue analysis. An analysis of variance (ANOVA) was conducted with $p < 0.05$ followed by Tukey`s HSD (honesty significant difference) test (*$p \le 0.05$, **$p \le 0.01$, ***$p \le 0.001$, ****$p \le 0.0001$) following Hasler and Horton (2008) to evaluate the differences between loam and the loam-residue-mixture in air capacity, AC, plant available water capacity, AWC, contact angle, CA, volume shrinkage index, ΔV and their interaction terms (two- fold and three-fold), respectively. The coefficient of determination (r^2) was used as an index for the goodness of fit.

RESULTS

Soil water retention characteristics after application of organic residues

The soil material before application of organic residues was classified as loam following FAO (2006) with 550 g kg^{-1} sand, 300 g kg^{-1} silt, and 150 g kg^{-1} clay and an organic carbon content of 12 g kg^{-1}, and weak acidic pH value of 6.8. The applicated organic residues are characterised by alkaline pH values between 7.5 and 8.1 (Table 1) and nitrogen contents between 1.2 and 4.0 kg m^{-3}.

The OC content of the loam was improved through organic residue application (12.4 g kg^{-1} up to 14.3 g kg^{-1}); there are small differences in pH values between 6.6 and 6.9, while compost application increases and digestate application decreases the pH value (Table 2).

Table 1. Basic properties considering pH values, dry matter, dm, and nitrogen, N_{total}, of shrub-derived compost (C), sewage sludge (S), and three digestates: (i) 80% maize and 20% sugar beet (80M20B), (ii) 20% maize and 80% sugar beet (20M80B), (iii) 20% winter wheat and 80% sugar beet (20W80B) with two repeated measurements each and symbol ± corresponds to the standard deviation.

Parameters	C	S	80M20B	20M80B	20W80B
pH_{CaCl2} (–)	8.1 ± 0.6	7.5 ± 0.3	7.7 ± 0.3	7.7 ± 0.3	7.8 ± 0.4
dm (%)	52 ± 4	n.a.	5.5 ± 0.2	5.4 ± 0.3	5.4 ± 0.1
N_{total} (kg m^{-3} om^{-1})	1.2 ± 0.2	4.0 ± 0.3	2.8 ± 0.1	2.9 ± 0.2	2.3 ± 0.1

dm: dry matter, om: organic matter, n.a.: not analysed

Table 2. Soil characteristics considering pH values and organic carbon, OC, after the application of shrub-derived compost (C), sewage sludge (S), and three digestates: (i) 80% maize and 20% sugar beet (80M20B), (ii) 20% maize and 80% sugar beet (20M80B), (iii) 20% winter wheat and 80% sugar beet (20W80B) to the loam (L), mean values with two repeated measurements each and symbol ± corresponds to the standard deviation. AC = air capacity, AWC = available water capacity. Differences in mean values compared to loam were significant at $p < 0.05$ (*), < 0.01 (**), < 0.001 (***), < 0.0001 (****) for ANOVA.

Parameters	L	C	S	80M20B	20M80B	20W80B
pH_{CaCl2} (–)	6.79 ± 0.3	6.87 ± 0.3	6.75 ± 0.3	6.62 ± 0.4	6.59 ± 0.6	6.65 ± 0.3
OC (g kg^{-1})	12.4 ± 1.4	13.5 ± 1.9	12.2 ± 1.1	14.1 ± 1.7	14.3 ± 1.5	13.2 ± 1.2
AC (cm^3 cm^{-3})	0.149	0.166	0.168	0.152	0.203***	0.122
AWC (cm^3 cm^{-3})	0.145	0.115**	0.124	0.133	0.114****	0.149

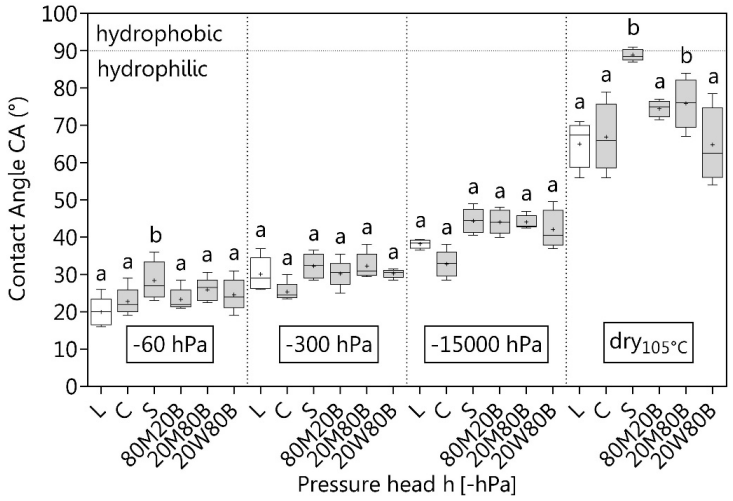

Fig. 3. Contact angles, CA, with 8–10 repeated measurements each at –60 hPa, –300 hPa, –15000 hPa and in dry stage (105°C). Different small letters indicate statistically differences in mean values at $p < 0.05$ for shrub-derived compost (C), sewage sludge (S), and three digestates: (i) 80% maize and 20% sugar beet (80M20B), (ii) 20% maize and 80% sugar beet (20M80B), (iii) 20% winter wheat and 80% sugar beet (20W80B) compared to the loam (L) for each stage, respectively.

The application of organic residues increased the air capacity of up to 0.203 cm^3 cm^{-3} for 20M80B while the plant available ater capacities decreased after application of organic residues, except for 20W80B (Table 2).

Soil wettability after application of organic residues

The loam and the added organic residues show contact angles, CA, > 0° and ≤ 90°, thus, the intact soil sample surfaces are characterised by subcritical hydrophilic conditions (Figure 3). The four dehydration stages show a relatively unique increase in CA through digestate application with no clear tendency between the differently composed digestates, while the sewage sludge is close to hydrophobic contact angles > 90° in the dry stage (105°C).

Shrinkage behaviour after application of organic residues

The loam-residue mixtures show comparatively higher void ratios than the untreated loam soil (Figure 4) and considering the maximum of the curve at the wet-side (ϑ_{shw}, e_{shw}) obtained with Eq. (9) (Table 3), the soil material shows a proportional volume and water loss with beginning of dehydration without structural shrinkage. The air entry point (ϑ_{ae}, e_{ae}), which separates the proportional shrinkage from the residual shrinkage indicates a more distinct residual than proportional shrinkage phase, except for loam and digestate (80M20B), respectively. The volume shrinkage indices indicated a low shrinkage tendency between 1.8% and 3.7%, while the loam-compost-mixture significantly increased the shrinkage tendency compared to the untreated loam.

The shrinkage model in Eq. (9) fitted the observed shrinkage data with r^2 between 0.97 and 0.99 (Table 3). The fitting pa-

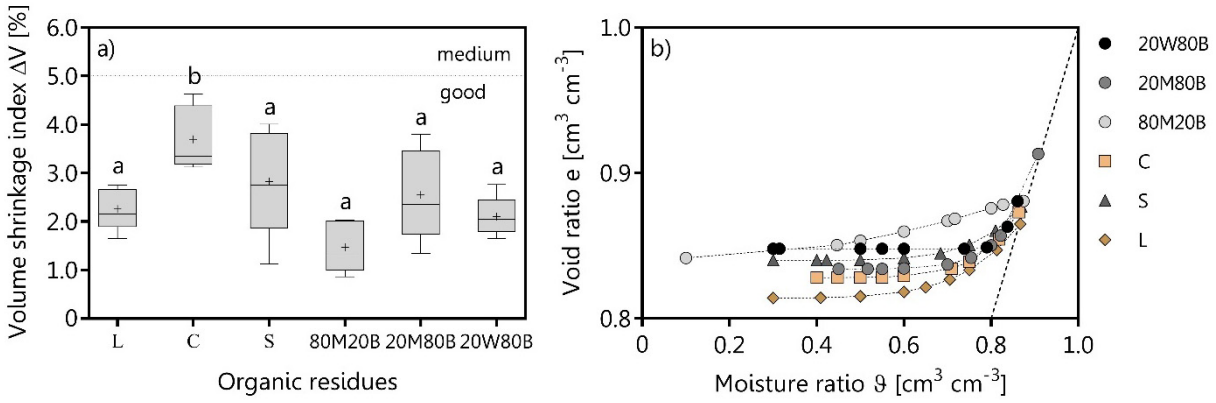

Fig. 4. a) volume shrinkage indices with boundary (ΔV = 5%) between good and medium shrinkage tendency and b) fitted shrinkage curves obtained by Eq. (9) after application of organic residues with 8–10 repeated measurements each (symbols). Different small letters indicate statistically differences in mean values at $p < 0.05$ for shrub-derived compost (C), sewage sludge (S), and three digestates: (i) 80% maize and 20% sugar beet (80M20B), (ii) 20% maize and 80% sugar beet (20M80B), (iii) 20% winter wheat and 80% sugar beet (20W80B) compared to the loam (L) for each stage, respectively.

Table 3. Parameter fits from the mean of 8–10 data points of the loam (L) and loam-residue-mixtures considering shrub-derived compost (C), sewage sludge (S), and three digestates: (i) 80% maize and 20 % sugar beet (80M20B), (ii) 20% maize and 80% sugar beet (20M80B), (iii) 20% winter wheat and 80% sugar beet (20W80B) obtained with Eq. (9); χ, p, q are dimensionless fitting parameters, e_{shw} and ϑ_{shw} indicate void and moisture ratio at the transition between the structural and proportional shrinkage, e_{ae} and ϑ_{ae} indicate void and moisture ratio at the transition between the proportional and residual shrinkage. The coefficient of determination (r^2) was used as an index for the goodness of fit.

Parameter	χ (–)	p (–)	q (–)	r^2 (–)		e_{shw}, ϑ_{shw} ($cm^3\ cm^{-3}$)	e_{ae}, ϑ_{ae} ($cm^3\ cm^{-3}$)
L	1.137	479.6	0.014	0.99	ϑ	0.880	0.498
					e	0.870	0.843
C	1.153	714.8	0.014	0.98	ϑ	0.868	0.859
					e	0.875	0.869
S	1.137	609.7	0.014	0.97	ϑ	0.879	0.869
					e	0.881	0.877
80M20B	1.116	284.4	0.007	0.97	ϑ	0.896	0.579
					e	0.885	0.859
20M80B	1.097	889.5	0.014	0.99	ϑ	0.907	0.889
					e	0.913	0.895
20W80B	1.196	279.4	1.615	0.99	ϑ	0.846	0.833
					e	0.879	0.853

rameter χ was on a relatively low level and also nearly identical for loam and the loam-residue-mixtures, thus, the volume and water loss in the structural shrinkage phase and therefore the structural shrinkage phase itself was of minor importance in case of initially homogenized soil samples.

Relationship between wettability and shrinkage behaviour

In terms of the wettability, the results indicate a strong negative relationship between the contact angles, CA, and the shrinkage-derived moisture ratio, ϑ, of the loam and loam-residue-mixtures ($r^2 \geq 0.95$). The lower the moisture ratio the higher is the contact angle (Figure 5).

The linear functions in Figure 5 were used for predicting the contact angles, CA*, on the basis of the fitted moisture ratios, ϑ, and the results indicate a strong positive relationship between ΔCA* and Δϑ* values during proportional shrinkage phase (e_s–e_{ae}, ϑ_s–ϑ_{ae}) with r^2 of 0.98 and strong negative relationship between CA and ϑ values at transition point between proportional and residual shrinkage (e_{ae}, ϑ_{ae}) with r^2 of 0.93 (Figure 6). Thus, the more pronounced the proportional shrinkage phase and the lower the moisture ratio at beginning of the residual shrinkage phase, the higher is the contact angle.

DISCUSSION

Air capacity and plant available water capacity after application of organic residues

The results indicate higher organic carbon contents after application of organic residues of up to 14.3 g kg^{-1} compared to the untreated loam with 12.4 g kg^{-1} as proposed by Ojeda et al. (2015), while the lower OC content of sewage sludge is related to the thermal treatment of wastewater, whereby ammonia can be volatilized.

The results also indicate higher air capacities, AC, of up to 0.203 $cm^3\ cm^{-3}$ for digestate 20M80B compared to 0.149 $cm^3\ cm^{-3}$ of the untreated loam in Table 2 as hypothesised before. The increase in AC values is in agreement with findings of

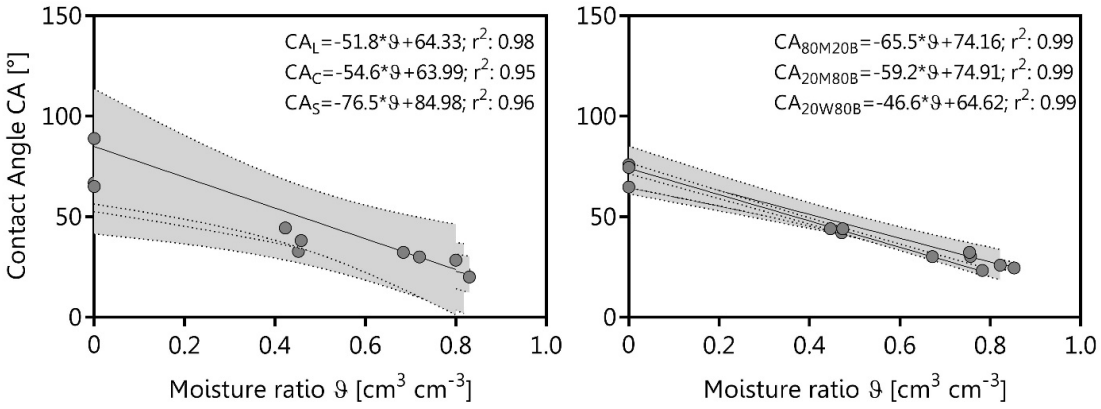

Fig. 5. Linear regression of mean values of observed contact angle, CA, and moisture ratios, ϑ, after application of shrub-derived compost (C), sewage sludge (S), and three digestates: (i) 80% maize and 20% sugar beet (80M20B), (ii) 20% maize and 80% sugar beet (20M80B), (iii) 20% winter wheat and 80% sugar beet (20W80B) compared to the loam (L). The r^2 indicates the coefficient of determination and the dashed lines indicate the confidence limits for a level of 95%.

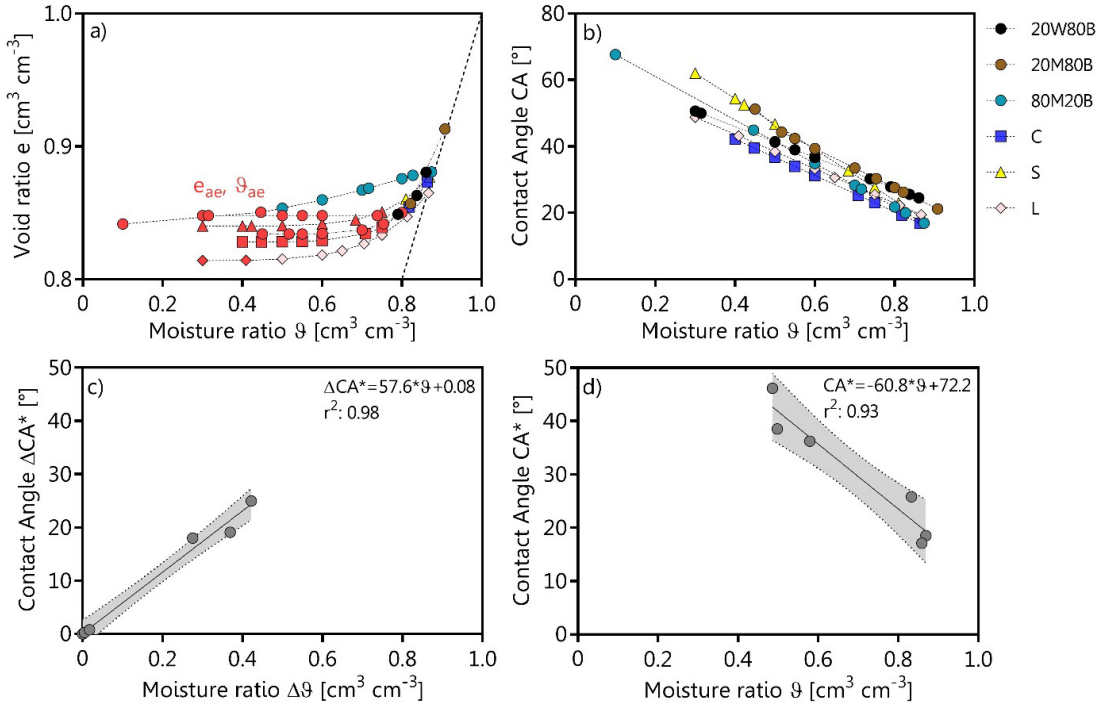

Fig. 6. a) fitted shrinkage curves on the basis of Eq. (9) with e_{ae} and ϑ_{ae} (red symbols) as transition points between proportional and residual shrinkage; b) contact angles, CA*, as function of fitted moisture ratios, ϑ, of shrub-derived compost (C), sewage sludge (S), and three digestates: (i) 80% maize and 20% sugar beet (80M20B), (ii) 20% maize and 80% sugar beet (20M80B), (iii) 20% winter wheat and 80% sugar beet (20W80B) and loam (L); c) change, Δ, of CA* and ϑ during proportional shrinkage phase (e_s–e_{ae}, ϑ_s–ϑ_{ae}); d) CA* values at transition point between proportional and residual shrinkage phase (e_{ae}, ϑ_{ae}) see Table 3. The r^2 indicates the coefficient of determination and the dashed lines indicate the confidence limits for a level of 95%.

Ojeda et al. (2015) and a positive effect on AC values was also shown for highly compacted soils ($\rho_b \geq 1.8$ g cm^{-3}), where the application of compost compensated low AC values (Jasinska et al., 2006; Beck-Broichsitter et al., 2018b). The plant available water capacities, AWC, in Table 2 were equal (20W80B) or lower than the AWC value of the untreated loam of 0.145 cm^3 cm^{-3} which is in contrast to findings of Beck-Broichsitter et al. (2018b).

Impact of organic residues on soil wettability

The results indicate that the contact angle of the untreated loam was not seriously affected by the organic-residue mixtures as hypothesized before, but with decreasing moisture ratios, ϑ, during dehydration of the soil samples from –60 hPa to oven-dried state, the CA values ranged between > 0° and < 90° and can be characterised as subcritical hydrophilic, resulting in a reduced wettability (Lamparter et al., 2006; Goebel et al., 2007).

It should be taken into account that the impact of the soil organic matter on the contact angles is less examined, while especially aliphatic and nonpolar C–H groups can make up a significant portion of the soil organic matter (Kodešová et al., 2012). Considering the potential wettability index analysis (PWI: C–H/C=O ratio) of Fér et al. (2016), these groups may lower the wettability on aggregate surfaces. However, the results of

Leue et al. (2015) indicate that the wetter the soil core surface, the less pronounced is the effect of SOM on surface contact angles and therefore the mm-scale variability of soil wettability (Hallett et al., 2004). In this case, the field situation with annual average pressure heads between –60 hPa and –300 hPa are realistic for agricultural-used topsoils, thus, there is only a less pronounced tendency pointing out the negative impact of applied organic residues on the soil surface wettability.

Interaction between shrinkage and wettability

The soil shrinkage curves are displayed only with proportional-, residual-, and zero-shrinkage phases that is typical for initially homogenized soil material (Beck-Broichsitter et al., 2018a; Peng and Horn, 2013). The results in Figure 4 indicate a low shrinkage tendency with ΔV values between 1.8% and 3.7% compared to ΔV values of 2.3% of landfill topsoil layer (0.05 m; 12 g kg^{-1} OC) after application of compost (Beck-Broichsitter et al., 2018a). Thus, the application of the presented organic residues not necessarily reduced the shrinkage crack formation tendency of untreated loam (ΔV = 2.2%) as hypothesized before (iii). The overall ΔV values < 5% in Figure 4 indicate a reduced shrinkage crack tendency of organic residues that can prevent deeper shrinkage cracks in drier periods (Horn et al., 2014) thus limiting the potential of preferential leaching of plant nutrients through soil macropores.

The shrinkage model of Peng and Horn (2005) fitted the observed void ratios, e, and moisture ratios, ϑ, well with $r^2 \geq 0.96$ in Table 3 and the contact angles were also well predicted through fitted ϑ values with $r^2 \geq 0.95$ (Figure 5). Therefore, it seems as if we can regression-based predict contact angles especially in the low moisture ratio range. The evaluation of the contact angles in the proportional shrinkage phase where a proportional loss in soil and water volume is assumed (i.e., Bradeau et al., 2004) is essential for ϑ values in the residual- and zero-shrinkage phase that is of major interest for the wettability of intact soil core surfaces (e.g, Goebel et al., 2007).

Thus, untreated loam and digestates consisting of maize and sugar beet are of special interest because of its more pronounced proportional shrinkage behaviour and reduced ϑ values in the dry range that may intensify the infiltration through shrinkage cracks in deeper soil layers (Gerke, 2012; Kodešová et al., 2011, 2012) compared to compost, sewage sludge and wheat-derided digestate (20W80B). In a positive way, intense shrinkage cracks can also reduce potential surface runoff and soil erosion by increasing infiltration (Horn et al., 2014).

CONCLUSION

The objective of the study was to determine the effect of application of digestates with different composition in maize, sugar beet and winter wheat, compost of shrub debris and sewage sludge on shrinkage behaviour and contact angle of till-derived loamy topsoil of a Haplic Luvisol under agricultural use.

The contact angle of the loam was not affected by application of the organic-residues, and the contact angles remained in the range between >0° and <90° indicating subcritical hydrophobic conditions, while the shrinkage crack formation tendency of untreated loam was not necessarily lowered. The combined determination of shrinkage behaviour and contact angles enabled a regression-based predicting of contact angels especially in the low moisture ratio range.

For a more quantitative relation between soil cracking, drying, and wettability, studies on the impact of shrinkage regime on wettability should focus on the finer-textured soils and include field conditions.

Acknowledgements. This research was supported by the Innovation Foundation Schleswig-Holstein and the ZMD Rastorf GmbH, Germany. The authors thank the technicians Ines Schütt and Sabine Hamann (University of Kiel) for supporting the soil chemical and physical analysis.

REFERENCES

Alaoui, A., Lipiec, J., Gerke, H.H., 2011. A review of the changes in the soil pore system due to soil deformation: A hydrodynamic perspective. Soil Till Res., 115–116, 1–15.

Bachmann, J., Woche, S.K., Goebel, M.O., 2013. Small-scale contact angle mapping on undisturbed soil surfaces. J. Hydrol. Hydromech., 61, 3–8.

Bebej, J., Homolák, M., Orfánus, T., 2017. Interaction of Brilliant Blue dye solution with soil and its effect on mobility of compounds around zones of preferential flows at spruce stand. Dent. Eur. For. J., 63, 79–90. DOI: 10.1515/forj-2017-0020.

Beck-Broichsitter, S., Gerke, H.H., Horn, R., 2018a. Shrinkage characteristics of boulder marl as sustainable mineral liner material of landfill capping systems. Sustainability, 10, 4025.

Beck-Broichsitter, S., Fleige, H., Horn, R., 2018b. Compost quality and its function as a soil conditioner of recultivation layers – a critical review. Int. Agrophys., 32, 11–18.

Beck-Broichsitter, S., Fleige, H., Gerke, H.H., Horn, R., 2020. Effect of artificial soil compaction in landfill capping systems on anisotropy of air-permeability. J. Plant. Nutr. Soil Sci., 1–11. DOI: 10.1002/jpln.201900281.

Braudeau, E., Frangi, J.P., Mothar, R.H., 2004. Characterizing non-rigid dual porosity structured soil medium using its characteristic SC. Soil Sci. Soc. Am. J., 68, 359–370.

Chen, P., Ning, L., 2018. Generalized equation for soil shrinkage curve. J. Geotech. Geoenviron., 144, 8, 04018046.

FAO, 2006. Guidelines for soil profile description. 4th edition. Land and water development division. Rome, Italy.

Fér, M., Leue, M., Kodešová, R., Gerke, H.H., Ellerbrock, R.H., 2016. Droplet infiltration dynamics and soil wettability related to soil organic matter of soil aggregate coatings and interiors. J. Hydrol. Hydromech., 64, 111–120.

Gerke, H.H., 2006. Preferential flow descriptions for structured soils. J. Plant Nutr. Soil Sci. 169, 382–400. DOI: 10.1002/jpln.200521955.

Gerke, H.H., 2012. Macroscopic representation of the interface between flow domains in structured soil. Vadose Zone J., 11, 3. DOI: 10.2136/vzj2011.0125.

Goebel, M.-O., Woche, S.K., Bachmann, J., Lamparter, A., Fischer, W.R., 2007. Significance of wettability-induced changes in microscopic water distribution for soil organic matter decomposition. Soil Sci. Soc. Am. J., 71, 5, 1593–1599.

Hallett, P.D., Nuna, N., Douglas, J.T., Young, I.M., 2004. Millimeter-scale spatial variability in soil water sorptivity: scale, surface elevation, and subcritical repellency effects. Soil Sci. Soc. Am. J., 68, 352–358.

Hartge, K.H., Horn, R., 2016. Essential Soil Physics. In: Horton, R., Horn, R., Bachmann, J., Peth, S. (Eds.): An introduction to soil processes, structure, and mechanics. Schweizerbart Science Publishers, Stuttgart, Germany, 391 p.

Hasler, M., Horton, L.A., 2008. Multiple contrast tests in the presence of heteroscedasticity. Biometrical J., 50, 793–800. DOI: 10.13140/RG.2.2.29821.36320.

Horn, R., Peng, X., Fleige, H., Dörner, J., 2014. Pore rigidity in structured soils – only a theoretical boundary condition for hydraulic properties? J. Soil Sci. Plant Nutr., 60, 3–14.

IUSS Working Group WRB, 2014. World reference base for soil resources 2006. 2nd ed. World Soil Resources Reports No. 103. FAO, Rome.

Jasinska, E., Wetzel, H., Baumgartl, T., Horn, R., 2006. Heterogeneity of physico-chemical properties in structured soils and its consequences. Pedosphere, 16, 284–296.

Kodešová, R., Jirků, V., Kodeš, V., Mühlhanselová, M., Nikodem, A., Žigová, A., 2011. Soil structure and soil hydraulic properties of Haplic Luvisol used as arable land and grassland. Soil Till. Res., 1112, 154–161.

Kodešová, R., Němeček, K., Kodeš, V., Žigová, A., 2012. Using dye tracer for visulization of preferential flow at macro- and microscales. Vadose Zone J., 11, 1–10.

Köhne J.M., Köhne, S., Simunek, J., 2009. A review of model applications for structured soils: b) Pesticide transport. J. Cont. Hydrol., 104, 36–60. DOI: 10.1016/j.jconhyd.2008.10.003.

Lamparter, A., Deurer, M., Bachmann, J., Duijnisveld, W.H.M., 2006. Effect of subcritical hydrophobicity in a sandy soil on water infiltration and mobile water content. J. Plant Nutr. Soil Sci., 169, 1, 38–46.

Leue, M., Gerke, H., Godow, S.C., 2015. Droplet infiltration and organic matter composition of intact crack and biopore surfaces from clay-illuvial horizons. J. Plant Nutr. Soil Sci., 178, 250–260.

Lu, N., Dong, Y., 2016. Correlation between soil shrinkage curve and water retention characteristics. J. Geotech. Geoenviron., 144, 8, 04017054.

Ojeda, G., Mattana, S., Àvila, A., Alcañiz, J.M., Volkmann, M., Bachmann, J., 2015. Are soil-water functions affected by biochar application? Geoderma, 249–250, 1–11.

Peng, X., Horn, R., 2005. Modeling soil shrinkage curve across a wide range of soil types. Soil Sci. Soc. Am. J., 69, 3, 584–592.

Peng, X., Horn, R., 2013. Identifying six types of soil shrinkage curves from a large set of experimental data. Soil Sci. Soc. Am. J., 77, 372–381.

R Development Core Team, 2014. R: A language and environment for statistical computing. R Foundation for Statistical Computing, Vienna, Austria.

Risberg, K., Cederlund, H., Pell, M., Arthurson, V., Schnürer, A., 2017. Comparative characterization of digestate versus pig slurry and cow manure – chemical composition and effects on soil microbial activity. Waste Manage., 61, 529–538.

Ruggieri, L., Artola, A., Gea, T., Sanchez, A., 2008. Biodegradation of animal fats in a co-composting process with wastewater sludge. Int. Biodeter Biodegr., 62, 3, 297–303.

Seyfarth, M., Holldorf, J., Pagenkemper, S.K., 2012. Investigation of shrinkage induced changes in soil volume with laser scanning technique and automated soil volume determination - A new approach/method to analyze pore rigidity limits. Soil Till. Res., 125, 105–108.

Voelkner, A., Holthusen, D., Horn, R., 2015. Influence of homogenized residues of anaerobic physicochemical properties of differently textured soils. J. Plant Nutr. Soil Sci., 178, 261–269.

Vogelmann, E.S., Reichert, J.M., Prevedello, J., Consensa, C.O.B., Oliveira, A.É., 2013. Threshold water content beyond which hydrophobic soil become hydrophilic. The role of soil texture and organic matter content. Geoderma, 209–210, 177–187.

Wang, X.Y., Zhao, Y., Horn, R., 2010. Soil wettability as affected by soil characteristics and land use. Pedosphere, 20, 43–54.

Received 14 October 2019
Accepted 31 January 2020